# Bioorthogonal Antigens

Pawlak, J.B.

# 4

# Towards imaging of bioorthogonal antigens throughout antigen cross-presentation

Joanna B. Pawlak, Daphne M. van Elsland, Anouk M.F. van der Gracht, Silvia Pujals Riatos, Nico J. Meeuwenoord, Marcel Camps, Colin Watts, Dmitri V. Filippov, Lorenzo Albertazzi, Herman S. Overkleeft, Ferry A. Ossendorp and Sander I. van Kasteren contributed to the work described in this chapter.

## 4.1 Introduction

The activation of cytotoxic T cells (CTLs) is one of the key events in adaptive immunity and essential for the clearance of viruses and cancers[1]. CTLs are activated by antigen presenting cells (APCs) in a process called antigen cross-presentation[2]. Cross-presentation involves uptake of antigen, followed by routing to a compartment where it can be loaded onto MHC-I[3]. During this routing, the antigen is proteolytically processed to liberate epitope peptides that are loaded onto MHC-I[4].

The use of traditional reporter strategies to study intracellular antigen routing has some limitations: the requirement of proteolysis for liberation of epitope peptides means that any amide-linked reporters must be disconnected from the peptide somewhere during routing. Furthermore, the chemical modification of sidechains with fluorophores can alter protease specificity, membrane crossing ability and solubility of the antigen[5]. In chapter 3 of this thesis bioorthogonal antigens were explored in their ability to determine surface levels of epitope peptides. To this end, minimal epitopes (which essentially do not require processing prior to loading and can be loaded by surface exchange[6]) were exchanged on cells and the modification chemistry to label these peptides was optimized.

This chapter describes the further exploration of these bioorthogonal antigens as reagents to study cross-presentation itself. In theory, their properties allow the unbiased imaging throughout the cross-presentation process: from uptake all the way through to the on-surface appearance of the epitope. Not only can they be loaded into the MHC-Is and can the fluorophores be ligated following the loading (see Chapter 3), but the chemical stability of (at least some) bioorthogonal functionalities[7] could prevent their sequestration after uptake: fluorescence quenching due to the oxidative[8], reductive[9] and acidic conditions[10] found during antigen cross-presentation does not occur if the fluorophore is introduced after fixation. Secondly, their incorporation as sidechains of single amino acids would keep them intact even during the proteolytic degradation that degrades/disconnects other amide-based reporters.
A third property that was hypothesized to be favorable for the study of antigen processing and presentation was that the bioorthogonal groups are very small compared to fluorophores and can be incorporated isosterically and isocoulombically: the similar size and identical charge compared to natural amino acids results in minimal structural interference. This is postulated to minimize the effect on the rate of proteolysis. This is unlike, for example modification of lysines with small molecule fluorophores which alters the charge of the protein, the lipophilicity and subsequent rates of proteolysis[11].

## 4.2 Results and discussion

The aim of the work in this chapter was to therefore explore whether the bioorthogonal epitopes could be used in the context of longer antigens as reagents to study the intracellular mechanisms of cross-presentation and finally the on-surface appearance.

### Design of the bioorthogonal antigens

The aim was to use antigens with only a single bioorthogonal group at defined positions within the epitope, analogous to the minimal bioorthogonal epitopes used in chapter 3 of this thesis. The ideal reagent for this work would be a whole, folded protein antigen carrying a single modification at a controllable position within the epitope peptide (or elsewhere in the protein) for which here are two approaches available to obtain it: amber codon suppression[12] and methionine removal combined with auxotrophic methionine analogue incorporation[13].
The first approach makes use of an expanded genetic code, whereby *E.coli* cells are transformed with a $^{t}$RNA capable of recognizing the amber stop-codon and a $^{t}$RNA-synthetase capable of loading this $^{t}$RNA with an amino acid containing a bioorthogonally-modified amino acid. The second approach makes use of the fact

that certain strains of *E. coli* are auxotrophic for methionine, that is they do not biosynthesize their own methionine[14]. Depleting these cells of methionine allowed the replacement with a structural analogue of methionine[15]. Early examples of this use were the incorporation of heavy atoms (selenium) for crystallization[16], or other non-natural sidechains[13b, 17] as well as bioorthogonal methionine analogues azidohomolalanine (AHA) and homopropargylglycine (HPG)[18]. Davis and co-workers used this approach in combination with isosteric amino acid substitution (Met → Ile) to site-selectively modify proteins with single bioorthogonal groups and quantitatively ligating these using the same copper-catalyzed Huisgen reaction as described in chapter 3[13a, 19].

However, for the initial exploration of bioorthogonal antigens for cross-presentation studies, a simpler, more versatile, approach was chosen: solid-phase synthesis[20] that would allow the rapid production of differentially modified antigens. The advantage of this method over the above approaches is the ease with which diversity can be introduced, due to the rapid rate at which these peptides can be synthesized. The downside is that the peptides likely lack secondary/tertiary structures. However, they have been shown to be relevant for immune system studies. Synthetic long peptide (SLP) antigens – as the ones proposed for use in this chapter – are making strong headway in the clinic for use in anti-cancer vaccines[21]. They are also potent activators of CD8 CTLs, which highlights their ability to be cross-presented[22]. A series of SLPs carrying bioorthogonal groups within their epitopes were thus designed to explore the use of these bioorthogonal antigens in this complex setting of cross-presentation.

In chapter 3 it was shown that the ligation reaction of a Propargylglycine (Pg) modified HSV-$Gp_{498\text{-}505}$ peptide resulted in the most significant signal to noise ratio compared to other peptides tested. Therefore it was decided to synthesize a series of HSV-Gp synthetic long peptides. The sequence of these SLPs was designed based on the flanking regions of this minimal epitope[23]. Two variants were made based on long peptides that had previously been shown to show robust cross-presentation *in vitro*[22]. The first of these was an N-terminally extended peptide with the C-terminus being the end of the epitope as this peptide does not require processing by the proteasome (which is responsible for C-terminal liberation[24]) (Table 1, entry 1). The second peptide that was synthesized did carry a C-terminal extension ($A_5K$), which has been used in previous work by Khan *et al.*[22]. This peptide does require proteasomal processing to release the epitope (Table 1, entry 2).

These wild type peptides were also substituted with Pg-residues at position P4 or P7 within the epitope (Table 1, entries 3, 4 and 5) since these were shown in chapter 3 to be the most ligatable positions within this epitope.

| *Entry* | *Peptide Sequence* | *Peptide Name* | *Based on ovalbumin model peptide sequence* |
|---|---|---|---|
| 1 | NASVERIKTTSSIEFARL | HSV-$Gp_{488-505}$ | DEVSGLEQLESIINFEKL ($OVA_{247-264}$) |
| 2 | NASVERIKTTSSIEFARLAAAAAK | HSV-$Gp_{488-505}A_5K$ | DEVSGLEQLESIINFEKLAAAAAK ($OVA_{247-264A5K}$) |
| 3 | NASVERIKTTSSIEFA**Pg**L | HSV-$Gp_{488-505}$-Pg-7 | |
| 4 | NASVERIKTTSS**IPg**FARLAAAAAK | HSV-$Gp_{488-505}A_5K$ -Pg-4 | |
| 5 | NASVERIKTTSSIEFA**Pg**LAAAAAK | HSV-$Gp_{488-505}A_5K$ -Pg-7 | |

**Table 1.** Overview of HSV-Gp synthetic long peptides used in this study.

## T cell activation of HSV synthetic long peptides

The first aspect of these HSV-SLPs that was assessed was the ability of the non-bioorthogonal parent sequences to activate the HSV-$Gp_{498-505}$-specific, *Lac*Z-inducible T cell hybridoma HSV2.3.2E2[25]. This was to confirm that these peptides were indeed cross-presented and would thus serve as suitable models for the imaging of routing inside APCs. T cell activation of the non-bioorthogonal peptides as well as their Pg-modified variants was examined through monitoring of the β-galactosidase-mediated conversion of a fluorogenic substrate[22, 26] (Figure 1).

The first of these T cell activation assays were performed in the laboratory of Prof. Colin Watts at the University of Dundee (by Prof. Watts himself; Figure 1). There, bone marrow-derived dendritic cells[27] were incubated with the HSV-$Gp_{488-505}$ and -Pg-7 synthetic long peptides at the indicated concentrations followed by wash with medium and finally by addition of the HSV-specific T cell hybridomas[22]. Both the minimal epitope (HSV-$Gp_{498-505}$) as control and C-terminally extended peptide (HSV-$Gp_{488-505}$) could activate the T cell clone, proving this peptide to be suitable to study cross-presentation. The propargylated epitope did not activate the HSV2.3.2E2-clone at any of the tested concentrations (Figure 1).

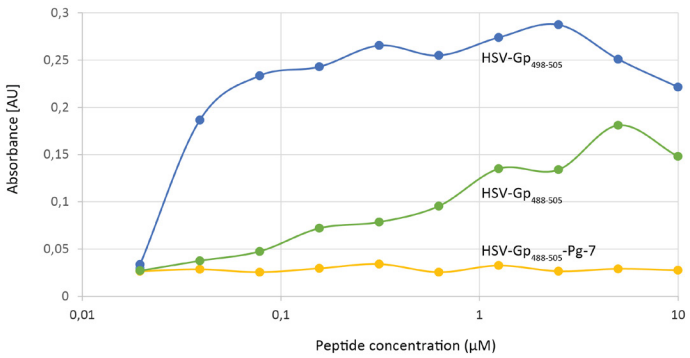


**Figure 1.** *Reactivity of the HSV peptides with the SSIEFARL-specific T cell clone HSV2.3.2E2. Only the non bioorthogonal controls - the HSV-$Gp_{498-505}$ and* HSV-$Gp_{488-505}$ *were recognized by the T cells.*

**Cellular uptake of bioorthogonal synthetic long peptides**

As the bioorthogonal variant of HSV-$Gp_{488\text{-}505}$ was not recognized by the cognate T cells, its suitability for studying cellular uptake was instead assessed using ccHc-ligation reaction. The uptake of HSV-$Gp_{488\text{-}505}$-Pg-7 was measured using Alexa Fluor-488 azide in ccHc-ligation conditions (as optimized in Chapter 3) after cells were fixed (Figure 3A). A pulse chase experiment using flow cytometry was conducted first: HSV-$Gp_{488\text{-}505}$-Pg-7 as well as its non-bioorthogonal control were incubated with the dendritic-cell line D1[28] for a fixed pulse (1h) followed by different chase periods. At the end of each chase period, the cells were fixed and exposed to ligation using AF-488 azide (Figure 3B). Use of a permeabilizing agent (saponin) proved unnecessary as cells became permeable to ccHc-reagents and Alexa Fluor-488 azide after fixation (Figure 2).

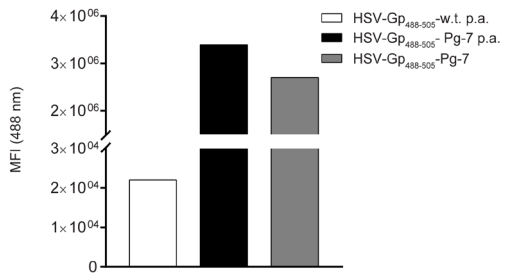


**Figure 2.** *D1s were pulsed for 5h with HSV-$Gp_{488\text{-}505}$ w.t. and HSV-$Gp_{488\text{-}505}$-Pg-7 (both 50 µM). ccHc was performed after fixation and permeabilization using permealizing agent (p.a.) - saponin (0.1 %). No significant improvement of the fluorescent signal was observed after addition of p.a. The fluorescent signal of AF-488 was assessed by quantification of the mean fluorescence intensity (MFI) at 488 nm using flow cytometry.*

As depicted in figure 3B, the fluorescent signal obtained from AF-488 azide peaked after the 1-hour pulse and showed time-dependent decay afterwards.

As a second assay to determine whether 1 hour was the optimal pulse-length for uptake, confocal microscopy was used to image this event. D1 cells were incubated with HSV-$Gp_{488\text{-}505}$-Pg-7 (50µM) for different time periods, both short (5, 15, 30, 45 minutes and 1 h; Figure 3C) and longer (1h, 3h, 5h, 8h; Figure 3D), then the cells were washed, fixed and reacted with AF-488 azide. Confocal images revealed a non-homogeneous fluorescent signal detectable from one hour onwards.

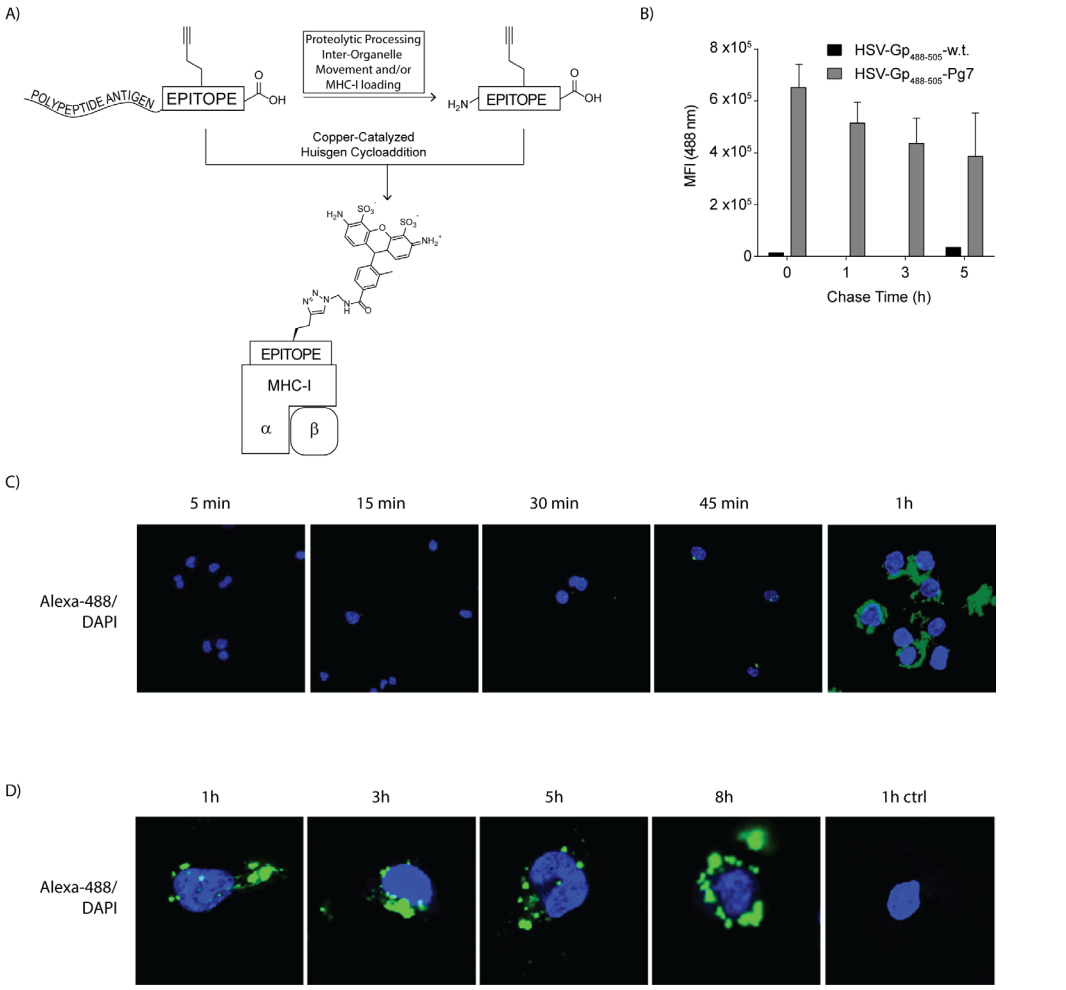


**Figure 3.** *Cellular uptake of the bioorthogonal synthetic long peptide (HSV-Gp$_{488-505}$-Pg-7). A) Overview of the approach: synthetic long peptides carrying bioorthogonal handles within their epitope are incubated with the D1-dendritic cell-line. At the end of the pulse chase experiments the cells are fixed and exposed to the bioorthogonal ligation reaction using AF-488. B) Flow cytometry of a pulse-chase experiment using HSV-Gp$_{488-505}$-Pg-7 (50μM) showed the uptake followed by a slow decay over time. Assay was set up in triplicate. All error bars correspond to SD of the mean. C) Confocal images revealed no fluorescent signal detectable after incubation shorter than one hour. D) Incubation at longer time periods resulted in the presence of a non-homogeneous fluorescent signal.*

To provide further insights into the uptake of this peptide, bioorthogonal correlative-light electron microscopy (CLEM)[29] imaging was performed. D1 cells were pulsed with HSV-Gp$_{488-505}$-Pg-7 (50μM) for 5 hours followed by wash and fixation. Subsequently, these samples were labeled with Alexa Fluor-488-azide. After the labeling, the samples were cryo-sectioned then transferred to an EM grid and finally imaged using confocal microscopy. After confocal imaging, sections were embedded in methyl cellulose with uranyl acetate and subjected to EM imaging. Images were correlated and morphological information obtained from the EM images has revealed

a patchy pattern of fluorescent signal located largely at or near the plasma membrane of the cells (Figure 4).

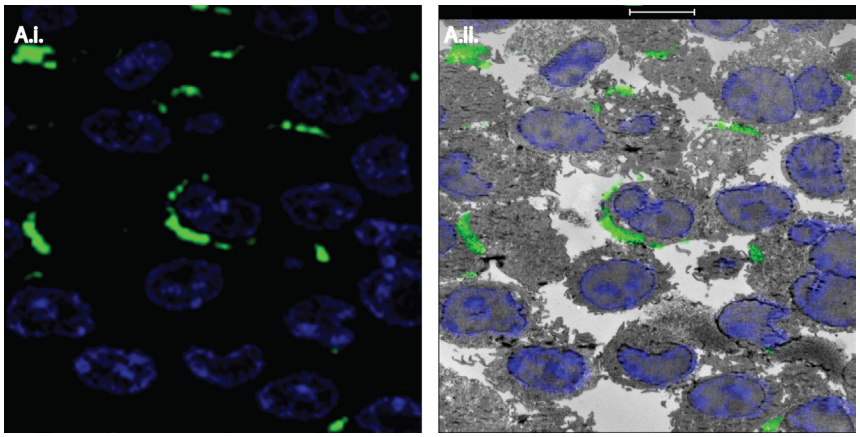


**Figure 4.** *CLEM imaging of the D1s cells incubated with* HSV-$Gp_{488\text{-}505}$-Pg-7 *(50μM) followed by wash with medium complete and PBS. Cells were fixed and labeled with Alexa Fluor-488-azide using ccHc-conditions (green). DAPI (blue) staining was used for correlation purposes; Samples were subjected to Tokuyasu sample preparation and cryosectioned into 75 nm sections*[29]*. A.i.) High magnification confocal image (green channel; AF-488). A.ii.) CLEM image of A.i. correlated with EM image; Scale bar 5μm.*

In order to determine more accurate location of the fluorescent signal, CLEM imaging at higher magnification was performed. The images have shown presence of large aggregates of the fluorescent signal located predominantly at or near the plasma membrane (Figure 5).

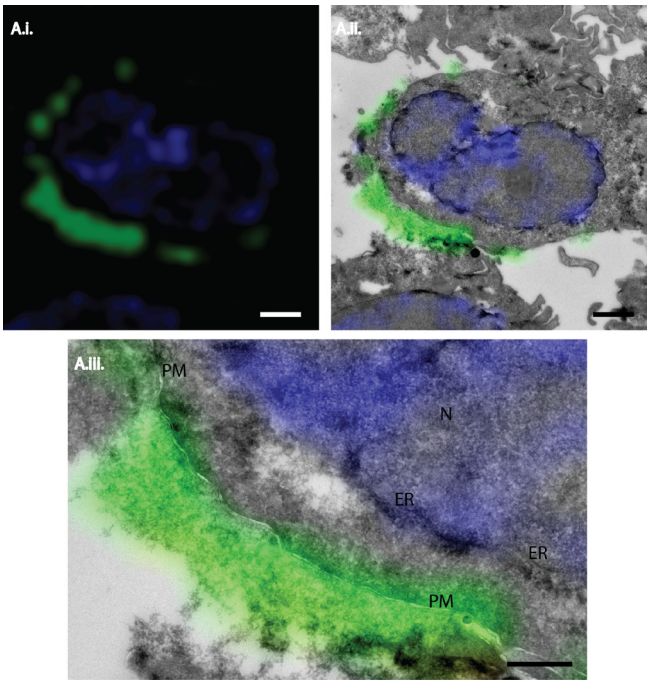


**Figure 5.** *CLEM imaging of the D1s cells incubated with* HSV-$Gp_{488\text{-}505}$-Pg-7 *(50μM) followed by wash with medium complete and PBS. Cells were fixed and labeled with Alexa Fluor-488-azide using ccHc-conditions (green). DAPI (blue) staining was used for correlation purposes; Samples were subjected to Tokuyasu sample preparation and cryosectioned into 75 nm sections*[29]*. A.i.) High magnification confocal image of AF-488 (green channel); Scale bar 1μm. A.ii.) CLEM image of A.i. correlated with EM image; Scale bar 1μm. A.iii.) Detail of A.ii, PM=plasma membrane, ER= endoplasmic reticulum, N=nucleus. Scale bar 500nm.*

These experiments have led to a hypothesis that HSV-$Gp_{488\text{-}505}$-Pg-7 aggregates and that these aggregates are either slowly internalized, perhaps serving as an antigen depot[30] or are not internalized at all. More research is needed to fully elucidate the behavior of these peptides in regard to solubility and T cell activation.

Taken together, these preliminary results demonstrate a potential of bioorthogonal SLPs as a tool to study cellular uptake using Alexa Fluor-488 azide in the ccHc reaction. However, an optimal bioorthogonal SLP model should first be synthesized and assessed and perhaps the switch to intact, folded, soluble bioorthogonal proteins should be made.

**Selective cell surface labeling of bioorthogonal synthetic long peptides**

After establishing the use of bioorthogonal antigens to image uptake, it was next attempted to use the approach to selectively ligate the processed peptide appearing on the cell surface. As fixing rendered the cells permeable to ccHc-reagents, the three-step labeling approach outlined in the latter part of Chapter 3 was explored to see whether it was sufficiently cell-surface restricted to only label this pool of the peptide (which is vastly smaller than the total intracellular pool).

To prevent labeling of cell-surface bound aggregates (which would give false positives), the switch was made to the more soluble SLP (Table 1, entry 2) carrying a C-terminal extension of 5 alanines and a lysine residue, which was less prone to aggregation than peptide (Table 1, entry 3). This extension had previously been shown to enhance solubility of other epitopes[22, 31]. HSV-$Gp_{488\text{-}505}A_5$K-Pg-4 and –Pg-7 (Table 1, entries 4 and 5 respectively) were thus used as bioorthogonal substitutes for the poorly soluble HSV-$Gp_{488\text{-}505}$-Pg-7 (Table 1, entry 3). The T cell assays of these doubly extended peptides showed the wild-type to be efficiently cross-presented (and again the bioorthogonal variant failed to induce T cell activation) (Figure 6).

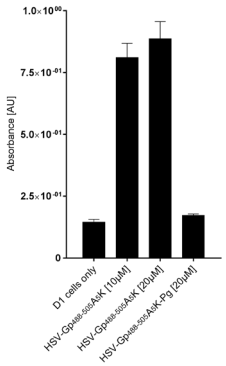


**Figure 6.** *Reactivity of the HSV peptides with the SSIEFARL-specific T cell clone HSV2.3.2E2. Only the non bioorthogonal control - the* HSV-$Gp_{488\text{-}505}A_5$K *was recognized by the T cells.*

The same bioorthogonal three-step labeling protocol as outlined in chapter 3 was applied to these two bioorthogonal SLPs to determine whether they could be labeled on-surface only in this case using an epi-fluorescence microscopy and flow cytometry. For the microscopy imaging, DC2.4 cells were incubated with the HSV-$Gp_{488\text{-}505}A_5$K-Pg-4 and –Pg-7 and with their non-bioorthogonal control for ~5 hours after which the cells were washed with medium, fixed and subjected to the three- step labeling. The images revealed an intracellular fluorescent signal obtained from Alexa Fluor-488 (Figure 7). Unfortunately, the Alexa Fluor-647 (from the three-step protocol) was not exclusively located at the cell surface. The bulk of the material showed non-homogeneous punctate staining that overlapped in part with the Alexa Fluor-488 intracellular stain. This suggested that for these experiments where the bulk of the peptide resided within the cell, even three-step labelling was insufficient to selectively label the extracellular pool.

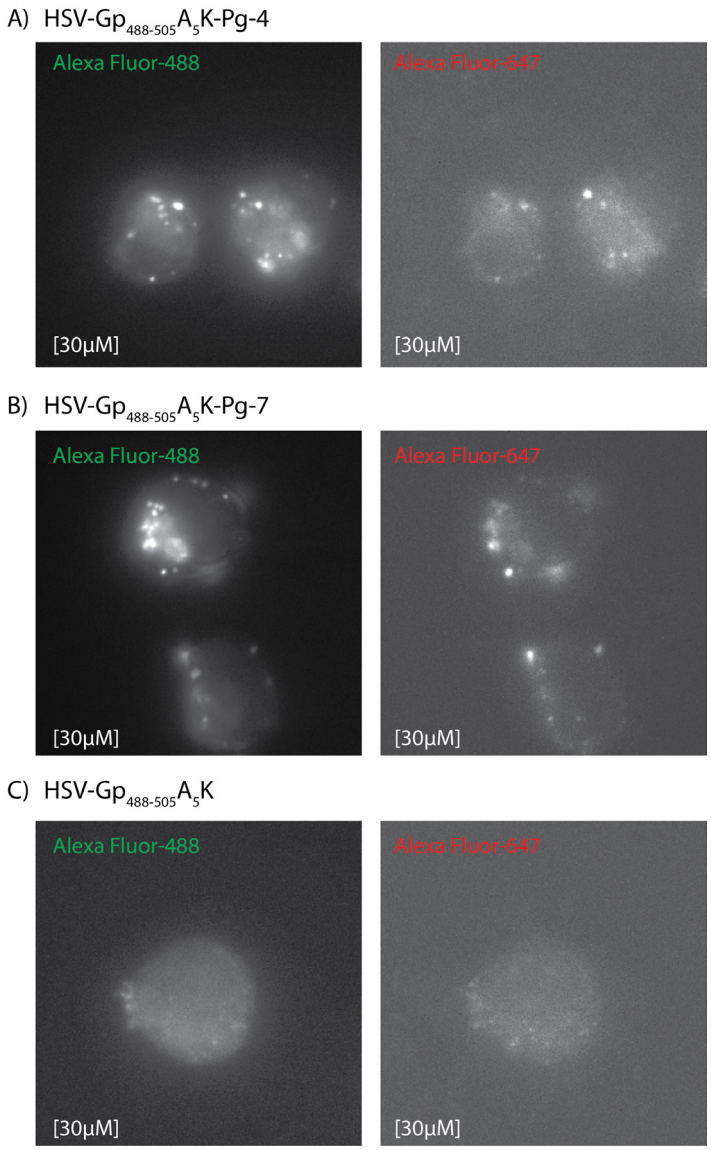


***Figure 7.*** *Epi-fluorescence illumination phase with white-light microscopy images of A) HSV-Gp$_{488-505}$A$_5$K-Pg-4 at 30µM as well as B) HSV-Gp$_{488-505}$A$_5$K-Pg-7 at 30µM showed not-substantial but visible signal to noise ratio as compared to their C) non-bioorthogonal control. DC2.4 were incubated with the indicated peptides for ~5h followed by wash with medium complete, fixation and exposure to the three- step labeling as described above.*

To assess whether the punctate staining was actually intracellular, an acid-strip experiment was performed whereby MHC-bound peptides are removed from the cell surface of the APC with mild acid[32]. If the signal from the Alexa Fluor-647 disappears after this acid strip, this would indicate that the observed peptide was indeed extracellular.

First, the completeness of the acid strip experiments was assessed using the T cell against the HSV-Gp$_{498-505}$-epitope. D1 cells were incubated with the HSV-Gp$_{488-505}$A$_5$K-

Pg-7 (20µM final concentration) and without the peptide (control) for 1,5h at 37°C. Followed the incubation, D1 cells were either washed with medium or gently fixed to prevent further processing and possible reuptake of the peptides. Alternatively, the peptides were exposed to mild acid elution, which results in the removal of cell surface proteins. After acid elution cells were either left to recover for ~5h at 37 °C to regenerate their peptide MHC-I complexes[33] or gently fixed. After the recovery time, the cells were mildly fixed and the SSIEFARL specific and MHC-I restricted cognate T cell clone (HSV2.3.2E2)[26] was added to all D1 cells. As a control to check whether the D1 cells after recovery were able to regenerate the MHC-I molecules, a MHC-I specific epitope SSIEFARL and no epitope (control) was added to these cells.

Next day, the epitopes were quantified by measuring the HSV T cell response as described above. T cell responses were observed in cells incubated with HSV-$Gp_{488-505}A_5K$ as well as after recovery (Figure 8A), but no T cell responses were observed in the D1 cells fixed directly after acid strip. Controls (T cell only as well as T cell only after incubation with the minimal epitope sample) were also negative (Figure 8B). These results strongly imply that the signal of presented epitope from HSV-$Gp_{488-505}A_5K$ can be abolished.

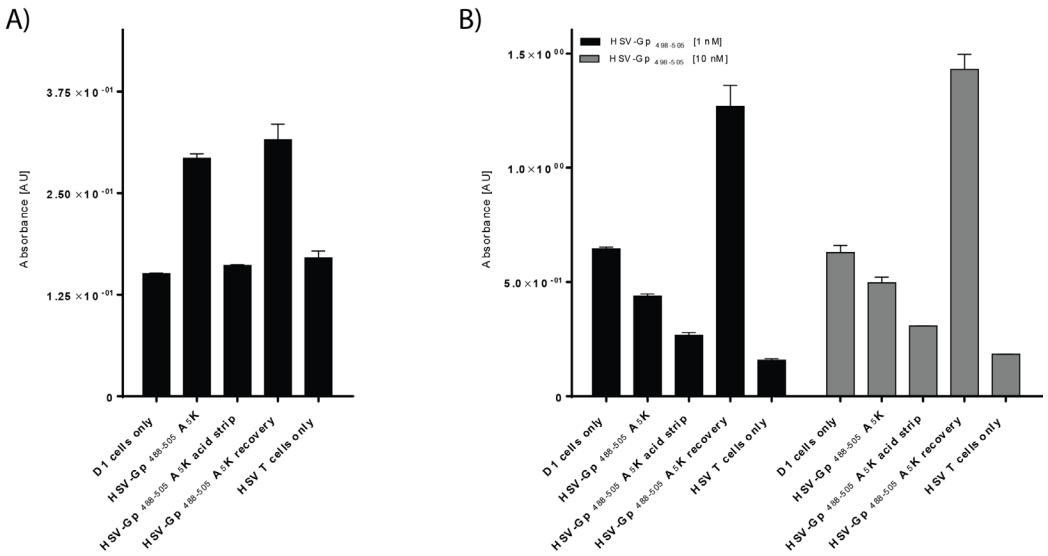


**Figure 8.** *Reactivity of the HSV-$A_5K$ peptide in acid elution treated and untreated D1 cells with the SSIEFARL-specific T cell clone HSV2.3.2E2. A) Acid strip treatment abolished T cell response which can be rescued after recovery time of approximately 5h at 37°C. B) T cell response after recovery and in the presence of the minimal epitope (SSIEFARL) is increased as compared to incubation with HSV-$A_5K$ only in the presence of SSIEFARL. Assay was set up in triplicate. All error bars correspond to SD of the mean.*

Interestingly, T cell reactivity was not only rescued after the recovery period, but it was increased after the addition of the epitope as compared to incubation with HSV-$Gp_{488\text{-}505}A_5K$ only after addition of the epitope (Figure 8B). This phenomenon could be explained by the reported enhancement of MHC-I regeneration after cell recovery in the presence of the minimal epitopes[34].

With this suitable stripping protocol in hand, it was checked whether the Alexa-647 signal in Figure 7 resulted exclusively from the cell surface pool of peptide, or whether some of the signal was background resulting from background permeation of the antibody and protein A.

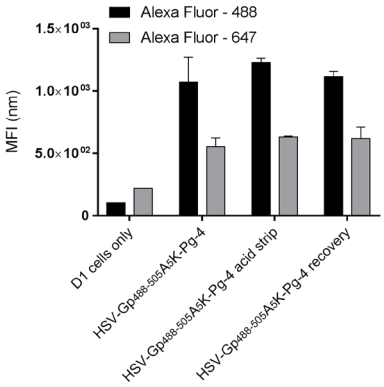


**Figure 9.** *Mean fluorescence intensity of Alexa Fluor-488 and -647 in acid elution treated and untreated D1 cells exposed to the three- step labeling. A substantial signal to noise ratio was not only observed in acid elution untreated cells and after recovery but also after acid strip treatment. Assay was set up in triplicate. All error bars correspond to SD of the mean.*

To assess this by flow cytometry, the D1s were incubated with HSV-$Gp_{488\text{-}505}A_5K$-Pg-4 and exposed to acid elution treatment as described above. The fluorescent signal of Alexa Fluor-488 and Alexa Fluor-647 was measured in acid elution treated and untreated cells. A substantial signal was observed in non-acid treated cells after recovery but also in acid elution treated cells (Figure 9).

The experiments in chapter 3 (Figure 12) showed that – despite an increase in small molecule penetrance, the cell's permeability to antibodies was not significantly affected after fixation and ccHc conditions. The data from Figure 9, however, indicate that the conditions of acid-strip, fixation followed by the ccHc-reaction could render the cells permeable to antibodies.

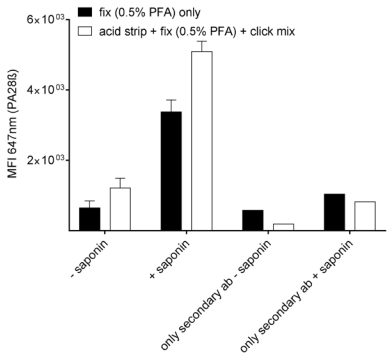


**Figure 10.** *The combination of exposure to acid strip treatment and ccHc conditions did permeabilized the D1 cells to antibody, which was assessed by quantifying the mean fluorescence intensity of the cytosolic antibody (PA28ß) in the presence and absence of the permeabilizing agent – saponin (0.1%). Assay was set up in triplicate. All error bars correspond to SD of the mean.*

This was next assessed by quantifying the mean fluorescence intensity of an antibody targeting a cytosolic region of the proteasomal protein (PA28β) in presence and absence of saponin. This was done for both acid stripped cells, as well as untreated cells. Indeed, it was observed that in the presence of both, acid elution and click mixture, the cells became partly permeable to the antibody (Figure 10).

These results excluded the use of acid strip-based protocols in combination with three-step labeling. Instead, in future, cells should either be incubated with bioorthogonal long peptides or gently fixed prior incubation to prevent peptide uptake and processing. If the bioorthogonal long peptides are taken up by the APCs, a fluorescent signal (obtained from three- step labeling) will be expected in cells that were incubated with long peptides prior to the gentle fixation and not in cells that were incubated with long peptides after they were mildly fixed. If this however is not the case it would be an indication for an aspecific adhesion of the peptides to the cell surface.

### 4.3 Conclusion

Bioorthogonal antigens are useful reagents to track the uptake of antigens. The one-step labeling approach indicates that the fed antigen is only minimally altered compared to wild-type antigens. This means there is less chance of artifacts stemming from other labeling techniques.

The three-step labeling presents a promising approach to selectively label the intracellular and extracellular pool of the bioorthogonal synthetic long peptides in a single experiment. However, the cell surface labeling still needs further research as it cannot be determined with these experiments whether the antigen labeled by the three-step approach is actually on the cell surface and loaded in an MHC-complex. In the future, using CLEM, intracellular (for example LAMP1 – lysosomal marker) and extracellular (for example MHC-I) markers should be combined with the three- step labeling method in order to provide an accurate antigen localization at a given time during cross-presentation process. This would also mean that (by studying co-localization with organelle markers), the relative contribution of the different proposed cross-presentation routes could be quantified in an unbiased manner, shedding light on this controversial and complex pathway[1, 3, 35].

## 4.4 Experimental section

**Reagents:**
Alexa Fluor-488 azide (catalogue number: A10266), Alexa Fluor-488 polyclonal antibody (catalogue number: A-11094) and Alexa Fluor-647-conjugated protein A (catalogue number: P21462) as well as donkey anti-goat IgG (H+L) secondary antibody, Alexa Fluor-647 (catalogue number: A-21447) were purchased from Thermo Fisher Scientific. PA28β antibody (catalogue number: SC-23642) was purchased from Santa Cruz biotechnology. Propargylglycine-Fmoc was purchased from Anaspec. Tris(3-hydroxypropyl-triazolylmethylamine) (THPTA) was purchased from Sigma-Aldrich, as were all other reagents at the highest available grade.

**Peptide synthesis:**
All peptides were synthesized using standard Fmoc Solid Support Chemistry and purified using high performance liquid chromatography (Prep column Gemini C18 110A 150x21.20 5µm) using 15 to 45 % gradient (A: 0.1% TFA in MilliQ H2O, B: ACN). LC-MS measurements were done on an API 3000 Alltech 3300 with a Grace Vydac 214TP 4,6 mm x 50 mm C4 column and analyzed by electrospray LC-MS analysis on a PE SCIEX: API 3000 LC/MS/MS system using a Gemini 3u C18 110A analytical column (5µ particle size, flow: 1.0 ml/min), on which the absorbance was also measured at 214 and 254 nm. Solvent system for LC-MS: A: 100% water, B: 100% acetonitrile, C: 1% TFA (aq).

**Cell culture:**
The D1 cell line, a long-term growth factor-dependent immature myeloid ($CD11b^+$, $CD8\alpha^-$) DC line of splenic origin, derived from a female C57BL/6 mouse was provided by M. Camps (Leiden University Medical Center) and was cultured as described previously[36]. When necessary, full maturation was achieved by adding Escherichia coli-derived LPS (serotype 026.B6; Sigma Aldrich) to the culture medium for 12h (final concentration 5µg/mL).
The DC2.4 cell line, an adherent C57BL/6 bone marrow derived DC line was kindly provided by Dr. Kenneth Rock (University of Massachusetts Medical School) and cultured as described previously[37].

**Mild acid stripping and HSV T cell assay:**
The D1s cells were incubated with respective peptides, at the indicated concentrations and times. After the incubation the cells were washed ones with medium complete and twice with PBS. The cells were either immediately fixed by adding 0.2% PFA in PBS for 15min at RT followed by double wash with PBS or mild acid treated essentially as described by Storkus *et. al*[32]. With the exception that D1 cell pellet was resuspended followed by addition of elution buffer (0.131 M Citric acid monohydrate, 0.061 M $Na_2HPO4{\cdot}2H_2O$ pH=3.3 adjusted with 5N NaOH or 5N HCl) for 60s at RT followed by addition of ice-cold medium complete. Cell suspension was then pelleted and washed with ice-cold PBS and either left at 37°C for ~5h in medium complete to recover or immediately fixed by adding 0.2% PFA in PBS for 15min at RT followed by double wash with PBS. At the end all D1 cells were plated in 96-well tissue-culture treated microtiter plate ($5x10^4$ cells/well) and HSV2.3.2E2 T cells ($5x10^4$ cells/well) were co-incubated for ~17h at 37°C. Stimulation of the HSV hybridoma was measured by a colorimetric assay using CPRG (chlorophenol red-β-D-galactopyranoside) as a substrate as described[22].

**Bioorthogonal ligation reaction using Alexa Fluor-488:**

**Flow cytometry:**

D1s were plated in 24-well tissue-culture treated plate ($5x10^5$ cells/well) and allowed to adhere for 1h at 37°C. The cells were incubated with respective peptides, at the indicated concentrations (usually 50µM) and times. After the incubation the cells were collected using 2mM EDTA in PBS, washed ones with medium complete and ones with PBS and transferred to Greiner v-bottom 96-well plate. The D1s were fixed by adding 50µl/well of 0.5% PFA in PBS for 1h at RT followed by double wash with PBS. The fixed D1s were then exposed to the bioorthogonal labeling mixture (1 mM $CuSO_4$, 10 mM sodium ascorbate, 1 mM THPTA ligand, 10 mM aminoguanidine, 100 mM HEPES, pH 8.4, Alexa Fluor-488-azide 5µM). After 1h at RT, the reaction mixture was aspirated and the cells were blocked with 1% BSA and 1% fish gelatin before being washed twice with PBS and analysis by guava easyCyte™ flow cytometry (Merck Millipore) and using FlowJo v10.1.

**Confocal microscopy:**

D1s were seeded ($7 \times 10^4$) on a 12-well removable chamber slide (Ibidi) and allowed to adhere for ~1h at 37°C. The cells were incubated with respective peptides, at the indicated concentrations (usually 50µM) and times. After the incubation the cells were washed ones with medium complete and ones with PBS. The D1s were fixed by adding ~150µl/well of 0.5% PFA in PBS for 1h at RT followed by double wash with PBS. The fixed D1s were then exposed to the bioorthogonal labeling mixture (1 mM $CuSO_4$, 10 mM sodium ascorbate, 1 mM THPTA ligand, 10 mM aminoguanidine, 100 mM HEPES, pH 8.4, Alexa Fluor-488-azide 5µM). After 1h at RT, the reaction mixture was aspirated and the cells were blocked with 1% BSA and 1% fish gelatin before being washed twice with PBS and DAPI stained for 5min at RT (final concentration 2µg/mL). After the staining procedures chambers were removed and cells were covered with a small drop of 50% glycerol after which a coverslip was mounted over the grid. Coverslips were fixed using Scotch Pressure Sensitive Tape. Samples were imaged with a Leica TCS SP8 confocal microscope (63x oil lens, N.A.=1.4).

**Correlation of light-electron microscopy (CLEM)**

The CLEM approach was adapted from van Elsland[29] *et. al*. Samples were prepared for cryosectioning as described elsewhere[38]. D1 cells were incubated with respective peptides, at the indicated concentrations (usually 50µM) and times. After the incubation the cells were washed ones with medium complete and ones with PBS. Cells were fixed and subjected to the bioorthogonal labeling as for confocal microscopy. After the labeling, cells were washed with PBS (3x) and were then fixed for 24h in freshly prepared 2% PFA in 0.1 M phosphate buffer. Fixed cells were embedded in 12% gelatin (type A, bloom 300, Sigma) and cut with a razor blade into 0.5 $mm^3$ cubes. The sample blocks were infiltrated in phosphate buffer containing 2.3 M sucrose for 3h. Sucrose-infiltrated sample blocks were mounted on aluminum pins and plunged in liquid nitrogen. The frozen samples were stored under liquid nitrogen.

Ultrathin cell sections of 75 nm were obtained as described elsewhere[29]. Briefly, the frozen sample was mounted in a cryo-ultramicrotome (Leica). The sample was trimmed to yield a squared block with a front face of about 300 x 250 µm (Diatome trimming tool). Using a diamond knife (Diatome) and antistatic devise (Leica) a ribbon of 75 nm thick sections was produced that was retrieved from the cryo-chamber with a droplet of 2.3 M sucrose. Obtained sections were transferred to a specimen grid previously coated with formvar and carbon grids were additionally coated with 100 nm FluoroSpheres (blue) carboxylate-modified (350/440) (Life Technologies).

Grids containing the thawed cryosections were left for 30 minutes on the surface of 2% gelatin in phosphate buffer at 37 °C. Grids were then washed with PBS, labeled with DAPI (final concentration 2µg/mL), and additionally washed with PBS and aquadest. Subsequently grids were washed with 50% glycerol and placed on a glass slides (pre- cleaned with 100% ethanol). Grids were then covered with a small drop of 50% glycerol after which a coverslip was mounted over the grid. Coverslips were fixed using Scotch Pressure Sensitive Tape. Samples were imaged with a Leica TCS SP8 confocal microscope (63x oil lens, N.A.=1.4).

After confocal microscopy the EM grid with the sections was remove from the glass slide, rinsed in distilled water and incubated for 5min on droplets of uranylacetate/methylcellulose. Excess of uranylacetate/methylcellulose was blotted away and grids were air-dried. EM imaging was performed with a Tecnai 12 Biotwin transmission electron microscope (FEI) at 120 kV acceleration voltages. Correlation of confocal and EM images was performed in Adobe Photoshop CS6. In Adobe Photoshop, the LM image was copied as a layer into the EM image and made 50 % transparent. Transformation of the LM image was necessary to match it to the larger scale of the EM image. This was performed via isotropic scaling and rotation. Interpolation settings; bicubic smoother. Alignment at low magnification was carried out with the aid of nuclear DAPI staining in combination with the shape of the cells; at high magnification alignment was performed using the fiducial beads.

**Permeability assay:**
D1s were collected using 2mM EDTA in PBS, fixed in 0.5% PFA in PBS for 1h at RT and exposed to the click cocktail mix (as described previously but without a fluorophore) for 1h at RT. After the wash, cells were permeabilized with 0.1% saponin in 1% BSA in PBS (control cells were incubated without saponin throughout whole experiment) for ~20min at RT followed by incubation with PA28β antibody (final concentration 2µg/mL) in 0.1% saponin in 1% BSA in PBS for 30min on ice followed by wash and incubation with the donkey anti-goat IgG (H+L) secondary antibody (0.5µg/mL) in 0.1% saponin in 1% BSA in PBS for 30min on ice followed by wash and analysis by Guava EasyCyte™ flow cytometry (Merck Millipore) and using FlowJo v10.1.

**The three- step labeling:**
The DC2.4 cells were incubated with respective peptides, at the indicated concentrations and times. After the incubation the cells were washed ones with medium complete and ones with PBS. The cells were fixed by adding 2% PFA in PBS for 20min at RT followed by double wash with PBS. The fixed DC2.4 were then exposed to the bioorthogonal labeling mixture (1 mM $CuSO_4$, 10 mM sodium ascorbate, 1 mM THPTA ligand, 10 mM aminoguanidine, 100 mM HEPES, pH 8.4, Alexa Fluor-488-azide 5µM). After 1h at RT, the reaction mixture was aspirated and the cells were blocked with 1% BSA and 1% fish gelatin before being washed twice with PBS. Next, the cells were incubated with an Alexa Fluor-488 antibody (final concentration 2µg/mL) in 100mM HEPES pH 7.2 supplemented with 1% BSA and 1% fish gelatin for 1h at RT. After the incubation, cells were washed with PBS and blocked with 1% BSA and 1% fish gelatin before being exposed to Alexa Fluor-647-conjugated protein A (final concentration 5µg/mL) for 20min at RT followed by PBS wash step and blocking with 1% BSA and 1% fish gelatin.

## 4.5 References


[1] J. Neefjes, M. L. Jongsma, P. Paul, O. Bakke, *Nat Rev Immunol* **2011**, *11*, 823-836.

[2] aO. P. Joffre, E. Segura, A. Savina, S. Amigorena, *Nat Rev Immunol* **2012**, *12*, 557-569; bM. J. Bevan, *The Journal of experimental medicine* **1976**, *143*, 1283-1288.

[3] J. S. Blum, P. A. Wearsch, P. Cresswell, *Annu Rev Immunol* **2013**, *31*, 443-473.

[4] K. L. Rock, D. J. Farfan-Arribas, L. Shen, *J Immunol* **2010**, *184*, 9-15.

[5] aM. Grammel, H. C. Hang, *Nat Chem Biol* **2013**, *9*, 475-484; bL. D. Hughes, R. J. Rawle, S. G. Boxer, *PLoS One* **2014**, *9*, e87649.

[6] J. B. Pawlak, B. J. Hos, M. J. van de Graaff, O. A. Megantari, N. Meeuwenoord, H. S. Overkleeft, D. V. Filippov, F. Ossendorp, S. I. van Kasteren, *ACS chemical biology* **2016**, *11*, 3172-3178.

[7] J. A. Prescher, C. R. Bertozzi, *Nat Chem Biol* **2005**, *1*, 13-21.

[8] in *Principles of Fluorescence Spectroscopy* (Ed.: J. R. Lakowicz), Springer US, Boston, MA, **2006**, pp. 277-330.

[9] S. Prashanthi, P. H. Kumar, L. Wang, A. K. Perepogu, P. R. Bangal, *Journal of fluorescence* **2010**, *20*, 571-580.

[10] J. Feitelson, *The Journal of Physical Chemistry* **1964**, *68*, 391-397.

[11] aC. P. Toseland, *Journal of Chemical Biology* **2013**, *6*, 85-95; bS. T. Larda, D. Pichugin, R. S. Prosser, *Bioconjug Chem* **2015**, *26*, 2376-2383.

[12] J. Normanly, L. G. Kleina, J. M. Masson, J. Abelson, J. H. Miller, *J Mol Biol* **1990**, *213*, 719-726.

[13] aS. I. van Kasteren, H. B. Kramer, H. H. Jensen, S. J. Campbell, J. Kirkpatrick, N. J. Oldham, D. C. Anthony, B. G. Davis, *Nature* **2007**, *446*, 1105-1109; bK. L. Kiick, D. A. Tirrell, *Tetrahedron* **2000**, *56*, 9487-9493.

[14] A. J. Doherty, S. R. Ashford, J. A. Brannigan, D. B. Wigley, *Nucleic Acids Res* **1995**, *23*, 2074-2075.

[15] Y. Ma, H. Biava, R. Contestabile, N. Budisa, M. L. di Salvo, *Molecules (Basel, Switzerland)* **2014**, *19*, 1004-1022.

[16] aH. Walden, *Acta Crystallographica Section D: Biological Crystallography* **2010**, *66*, 352-357; bJ. Sheng, Z. Huang, *International Journal of Molecular Sciences* **2008**, *9*, 258-271.

[17] aK. L. Kiick, R. Weberskirch, D. A. Tirrell, *FEBS Letters* **2001**, *502*, 25-30; bJ. C. M. Van Hest, K. L. Kiick, D. A. Tirrell, *Journal of the American Chemical Society* **2000**, *122*, 1282-1288.

[18] aA. J. Link, D. A. Tirrell, *Journal of the American Chemical Society* **2003**, *125*, 11164-11165; bK. L. Kiick, E. Saxon, D. A. Tirrell, C. R. Bertozzi, *Proceedings of the National Academy of Sciences of the United States of America* **2002**, *99*, 19-24.

[19] S. I. Van Kasteren, H. B. Kramer, D. P. Gamblin, B. G. Davis, *Nature Protocols* **2007**, *2*, 3185-3194.

[20] R. A. Houghten, *Proc Natl Acad Sci U S A* **1985**, *82*, 5131-5135.

[21] aG. G. Zom, D. V. Filippov, G. A. van der Marel, H. S. Overkleeft, C. J. Melief, F. Ossendorp, *Oncoimmunology* **2014**, *3*, e947892; bC. J. Melief, S. H. van der Burg, *Nature reviews. Cancer* **2008**, *8*, 351-360; c*Molecular Therapy* **2004**, *9*, 102.

[22] S. Khan, M. S. Bijker, J. J. Weterings, H. J. Tanke, G. J. Adema, T. van Hall, J. W. Drijfhout, C. J. Melief, H. S. Overkleeft, G. A. van der Marel, D. V. Filippov, S. H. van der Burg, F. Ossendorp, *J Biol Chem* **2007**, *282*, 21145-21159.

[23] M. J. Miley, I. Messaoudi, B. M. Metzner, Y. Wu, J. Nikolich-Zugich, D. H. Fremont, *J Exp Med* **2004**, *200*, 1445-1454.
[24] C. C. Oliveira, T. van Hall, *Frontiers in Immunology* **2015**, *6*, 298.
[25] S. Sanderson, N. Shastri, *Int Immunol* **1994**, *6*, 369-376.
[26] S. N. Mueller, C. M. Jones, C. M. Smith, W. R. Heath, F. R. Carbone, *J Exp Med* **2002**, *195*, 651-656.
[27] M. B. Lutz, N. Kukutsch, A. L. Ogilvie, S. Rossner, F. Koch, N. Romani, G. Schuler, *J Immunol Methods* **1999**, *223*, 77-92.
[28] C. Winzler, P. Rovere, M. Rescigno, F. Granucci, G. Penna, L. Adorini, V. S. Zimmermann, J. Davoust, P. Ricciardi-Castagnoli, *J Exp Med* **1997**, *185*, 317-328.
[29] D. M. van Elsland, E. Bos, W. de Boer, H. S. Overkleeft, A. J. Koster, S. I. van Kasteren, *Chemical Science* **2016**, *7*, 752-758.
[30] N. van Montfoort, M. G. Camps, S. Khan, D. V. Filippov, J. J. Weterings, J. M. Griffith, H. J. Geuze, T. van Hall, J. S. Verbeek, C. J. Melief, F. Ossendorp, *Proceedings of the National Academy of Sciences of the United States of America* **2009**, *106*, 6730-6735.
[31] J. L. Meek, *Proc Natl Acad Sci U S A* **1980**, *77*, 1632-1636.
[32] W. J. Storkus, H. J. Zeh, 3rd, R. D. Salter, M. T. Lotze, *J Immunother Emphasis Tumor Immunol* **1993**, *14*, 94-103.
[33] M. H. Fortier, E. Caron, M. P. Hardy, G. Voisin, S. Lemieux, C. Perreault, P. Thibault, *J Exp Med* **2008**, *205*, 595-610.
[34] aC. C. Oliveira, B. Querido, M. Sluijter, A. F. de Groot, R. van der Zee, M. J. Rabelink, R. C. Hoeben, F. Ossendorp, S. H. van der Burg, T. van Hall, *J Immunol* **2013**, *191*, 4020-4028; bE. D. Cram, R. S. Simmons, A. L. Palmer, W. H. Hildebrand, D. D. Rockey, B. P. Dolan, *Infect Immun* **2015**, *84*, 480-490.
[35] J. M. Vyas, A. G. Van der Veen, H. L. Ploegh, *Nat Rev Immunol* **2008**, *8*, 607-618.
[36] aD. H. Schuurhuis, S. Laban, R. E. M. Toes, P. Ricciardi-Castagnoli, M. J. Kleijmeer, E. I. H. van der Voort, D. Rea, R. Offringa, H. J. Geuze, C. J. M. Melief, F. Ossendorp, *The Journal of Experimental Medicine* **2000**, *192*, 145-150; bC. Winzler, P. Rovere, M. Rescigno, F. Granucci, G. Penna, L. Adorini, V. S. Zimmermann, J. Davoust, P. Ricciardi-Castagnoli, *The Journal of Experimental Medicine* **1997**, *185*, 317-328.
[37] aZ. Shen, G. Reznikoff, G. Dranoff, K. L. Rock, *J Immunol* **1997**, *158*, 2723-2730; bA. Rhule, B. Rase, J. R. Smith, D. M. Shepherd, *J Ethnopharmacol* **2008**, *116*, 179-186.
[38] P. J. Peters, in *Current Protocols in Cell Biology*, John Wiley & Sons, Inc., **2001**.